Inverting and non-inverting operation of InP microdisc modulators

J. Hofrichter, T. Morf, A. La Porta, B.J. Offrein, P. Mechet, G. Morthier, T. De Vries, H.J.S. Dorren and O. Raz

Reported is the inverting and non-inverting operation of indium phosphide (InP)-based microdisc modulators heterogeneously integrated on a silicon-on-insulator waveguide. The light transmitted through the waveguide can be modulated in an inverting and non-inverting manner depending on the bias conditions. Static extinction ratios and dynamic operation of the device up to 2.5 Gbit/s are demonstrated. Clean open eyes with extinction ratios better than 6 dB are shown and operation with a bit error rate below 1×10^{-10} is demonstrated at 1.0 Gbit/s for both operation modes with a bias of only 1 Vpp.

Introduction: Future computing and telecommunication systems demand an ever increasing input—output (IO) bandwidth and IO density, which can be met by integrated photonics. Besides light generation and light detection, the modulation of light is one of the key functionalities required for optical communication. Modulators based on the free-carrier plasma-dispersion effect and formed either as a disc [1], a ring [2] or as a Mach-Zehnder interferometer [3] have been investigated widely. Although most of these modulator concepts have been successfully demonstrated, their co-integration with other optical components, in particular laser sources, remains a challenge. Therefore, we have investigated the modulation properties of an InP microdisc modulator fabricated using a heterogeneous integration platform in which lasers [4], and wavelength converters [5], have been shown recently. Although basic modulation properties have also been observed for InP microdisc modulators [6], a quantitative evaluation of the modulation characteristics in terms of dynamic extinction ratio and BER remains to be demonstrated.

In this Letter, we report on two different operation modes of an InP microdisc modulator heterogeneously integrated on top of a silicon waveguide. We present static electrical and optical performance metrics, show dynamic operation up to 2.5 Gbit/s and demonstrate for the first time bit-error-free operation (BER lower than 1×10^{-10}) at 1.0 Gbit/s for both operation modes. In the experiments, the device was biased with voltage swings as low as 1.0 Vpp and can thus be directly driven with state-of-the-art CMOS electronics.

Device structure and fabrication: The device structure can be explained using the illustration in Fig. 1*a*. First, a 220×500 nm^2 silicon photonic waveguide is fabricated using optical projection lithography and dry etching. Then, a divinyl-tetramethyldisiloxane-benzocyclobutene (BCB) adhesive is spun on the silicon substrate and the InP substrate comprising the active multiple InAsP quantum well is bonded on top. After substrate removal, the III−V stack is structured using optical contact lithography, dry etching and lift-off to form an electrically contacted InP microdisk. Fig. 1*b* shows an optical microscope image of the microdisc modulator before the final metallisation step. The III−V microdisc cavity has a diameter of 8 μm, resulting in a footprint of only 50 μm^2. The silicon nanophotonic waveguide is evanescently coupled to the whispering gallery modes of the InP disc.

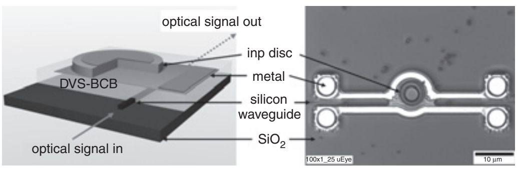

a *b*

Fig. 1 *Device structure of heterogeneously integrated InP microdisc modulator; silicon waveguide and silicon dioxide (SiO_2) cladding are indicated*

a Schematic illustration of devices
b Optical microscope image before final metallisation step

Light that is injected into the waveguide on one of the resonance wavelengths of the device will be modulated by the device either in an inverting or in a non-inverting manner, depending on the operation conditions.

Static characterisation: The characterisation was performed on a custom-made setup with automatically aligned fibre probes injecting polarisation-controlled light from a tunable laser into the waveguide using grating couplers. The device was biased electrically using a semiconductor device analyser. Fig. 2*a* shows the *I-V* characteristics of more than 30 microdisc modulators fabricated on the same chip. For zero bias, the measured current is within the noise and thus negligible.

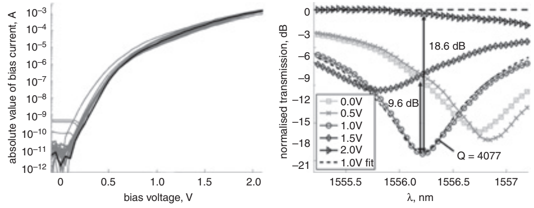

a *b*

Fig. 2 *Static characteristics of device*

a Static electrical *I-V*-characteristics of more than 30 microdisc modulators on same chip. Device investigated is highlighted
b Static optical transmission curves of measured device highlighted in Fig. 2*a* for positive bias voltages

At 1 V bias the current is about 10 μA and increases to 1 mA for 2 V bias voltage. To demonstrate low-power operation for potential on-chip applications with very limited supply voltage, we restricted the bias voltage swing to 1.0 Vpp. Also, it is desirable to have the functions of inverting and non-inverting modulation operation in the same device. By increasing the voltage from 0 to 1 V, the resonance wavelength of the device is blue-shifted because of the free-carrier plasma-dispersion effect, resulting in a drop of the static transmission by 9.6 dB at a wavelength of 1556.2 nm, as shown in Fig. 2*b*. Note that, although Fig. 2*b* displays the optical transmission characteristics for only one device, this behaviour was also observed for the other devices, but at a different wavelength because of fabrication variations slightly altering the diameter of the InP disc cavity. When increasing the bias voltage above the threshold voltage ($V_{th} = 1.5$ V) to 2 V, the resonance is strongly reduced because the microdisc is electrically pumped and the losses in the microdisc are reduced. In static operation, also the resonance is red-shifted because of thermal heating of the device (see Fig. 2*b*), which, however, is not the underlying principle of operation since the time constant is in the order of microseconds. For the operation wavelength of 1556.2 nm, the transmission increases by 18.6 dB, reducing the loss to 0.4 dB compared with the straight waveguide (Fig. 2*b*). For this wavelength, the transmission drops to the minimum value, thus indicating critical coupling. We fitted the maximal transmission dip with a simple ring resonator model and extracted a quality factor of $Q = 4077$. In summary, the device can be operated in inverting operation mode when biased between $V_{LO} = 0$ V and $V_{HI} = 1$ V and as a non-inverting modulator when driven with $V_{LO} = 1$ V and $V_{HI} = 2$ V.

Dynamic operation: We performed dynamic measurements to investigate the temporal behaviour of both operation modes. The sample was mounted on a thermoelectric cooler to stabilise the device temperature at 20°C and was directly driven by a 12.5 Gbit/s pulse pattern generator using a radio-frequency probe. Polarisation-controlled light from a tunable laser was coupled into and out of the chip by grating couplers and cleaved singlemode fibres. The transmitted optical signal was amplified by an erbium-doped fibre amplifier and spectrally filtered. We used a 10 Gbit/s photoreceiver for detection and electrically amplified the signal before measuring the bit error rate (BER) using a 12.5 Gbit/s error detector. The eye diagrams were recorded with a high-speed oscilloscope. For a non-return-to-zero pseudorandom binary sequence length of $2^{31} - 1$, error-free operation (i.e. operation with a BER lower than 1×10^{-10}) was achieved for both operation modes at 1.0 Gbit/s as shown in Fig. 3*a*. For the inverting and non-inverting operation mode a received power of −19.2 and −18.0 dBm, respectively, is required to recover the signal without errors.

As shown in Fig. 3*b*, the eye is clearly open for the inverting mode with a dynamic extinction ratio of 6 dB, whereas it appears slightly less open for the non-inverting mode with an extinction ratio of 8 dB (Fig. 3*c*). When biasing the disc between 1 and 2 V in the non-inverting operation mode, the lasing threshold is crossed resulting in slower rising and falling times as well as cross-gain modulation induced jitter, as the turn-on of the disc laser is pattern-dependent and affects the exact timing of resonance shift [7]. The jitter translates to the power penalty observed in Fig. 3*a*. For 2.5 Gbit/s, the operation could be demonstrated for the faster inverting operation mode. For a received optical power of −7 dBm, the BER is lower than 1×10^{-3}, which is sufficient for systems using forward error correction. Small-signal *S*-parameter measurements have shown a 3 dB bandwidth of 1.44 GHz for the inverting mode. The non-inverting mode exhibits 0.84 GHz, thus clearly indicating speed limitations for the operating mode based on the modulation of the losses in the disc cavity. If desired, the speed of the device could be further improved with the pre-emphasis technique [2].

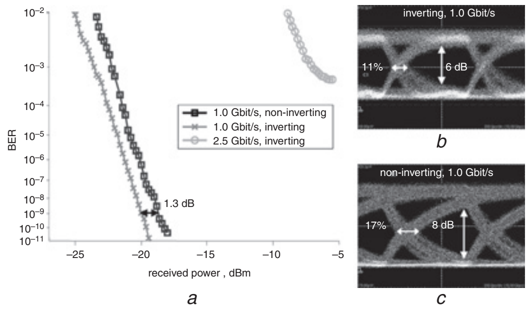

Fig. 3 *Dynamic measurements of InP microdisc modulator*

a Bit error rate measurements at 1.0 Gbit/s for inverting and non-inverting operation, and at 2.5 Gbit/s for inverting operation
b Eye diagram for inverting operation at 1.0 Gbit/s
c Eye diagram for non-inverting operation at 1.0 Gbit/s

Conclusions: We have demonstrated error-free operation at 1.0 Gbit/s of an InP microdisc heterogeneously integrated on top of an SOI waveguide as an electro-optical modulator. We have measured static electrical and optical performance figures. In the experiments a single InP microdisc modulator has been used as both an inverting and a non-inverting modulator with only 1 V bias, which allows the use of CMOS driver electronics. At 1.0 Gbit/s, operation with a BER lower than 1×10^{-10} was demonstrated for both modes with dynamic extinction ratios of 6 and 8 dB for the inverting and the non-inverting operation mode, respectively. Moreover, for the inverting operation mode of the modulator, we achieved operation at 2.5 Gbit/s with a BER lower than 1×10^{-3}, i.e. below the FEC limit. The device investigated in this Letter represents an interesting alternative to state-of-the-art modulator concepts because it combines compactness and very low drive voltage with flexibility in operation.

Acknowledgment: This work was supported by the European Union FP7–ICT project 'HISTORIC'.

6 March 2012
doi: 10.1049/el.2012.0684

J. Hofrichter, T. Morf, A. La Porta and B.J. Offrein (*IBM Research – Zurich, Säumerstrasse 4, Rüschlikon 8803, Switzerland*)

E-mail: jho@zurich.ibm.com

T. De Vries, H.J.S. Dorren and O. Raz (*COBRA Research Institute, Eindhoven University of Technology, PO Box 513, Eindhoven NL–5600 MB, The Netherlands*)

P. Mechet and G. Morthier (*Photonics Research Group, INTEC, Ghent University – IMEC, St.-Pietersnieuwstraat 41, Ghent 9000, Belgium*)

References

1 Watts, M.R., Zortman, W.A., Trotter, D.C., Young, R.W., and Lentine, A.L.: 'Vertical junction silicon microdisk modulators and switches', *Opt. Express*, 2011, **19**, (22), pp. 21989–22003
2 Xu, Q., Manipatruni, S., Schmidt, B., Shakya, J., and Lipson, M.: '12.5 Gbit/s carrier-injection-based silicon micro-ring silicon modulators', *Opt. Express*, 2007, **15**, (2), pp. 430–436
3 Rasigade, G., Ziebell, M., Marris-Morini, D., Fedeli, J.-M., Milesi, F., Grosse, P., Bouville, D., Cassan, E., and Vivien, L.: 'High extinction ratio 10 Gbit/s silicon optical modulator', *Opt. Express*, 2011, **19**, (7), pp. 5827–5832
4 Van Campenhout, J., Rojo-Romeo, P., Regreny, P., Seassal, C., Van Thourhout, D., Verstuyft, S., Di Cioccio, L., Fedeli, J.-M., Lagahe, C., and Baets, R.: 'Electrically pumped InP-based microdisk lasers integrated with a nanophotonic silicon-on-insulator waveguide circuit', *Opt. Express*, 2007, **15**, (11), pp. 6744–6749
5 Hofrichter, J., Raz, O., Liu, L., Morthier, G., Horst, F., Regreny, P., De Vries, T., Dorren, H.J.S., and Offrein, B.J.: 'All-optical wavelength conversion using mode switching in an InP microdisc laser', *Electron. Lett.*, 2011, **47**, (16), pp. 927–929
6 Liu, L., Van Campenhout, J., Roelkens, G., Soref, R.A., Van Thourhout, D., Rojo-Romeo, P., Regreny, P., Seassal, C., Fedeli, J.-M., and Baets, R.: 'Carrier-injection-based electro-optic modulator on silicon-on-insulator with a heterogeneously integrated microdisk cavity', *Opt. Lett.*, 2008, **33**, (21), pp. 2518–2520
7 Corzine, S.W., Tan, M.R., Wang, S.-Y., and Ding, G.: 'Modeling of turn-on delay time jitter in vertical-cavity surface-emitting lasers', HPL-95-136, Communications and Optics Research Laboratory